Revealing Polymorphic Phase Transformations in Polymer-Based Hot Melt Extrusion Processes

José R. Hernández Espinell[†,‡], **Vilmalí López-Mejías**[*,†,‡], **Torsten Stelzer**[*,‡,§]

[†]Department of Chemistry, University of Puerto Rico, Río Piedras Campus, San Juan, Puerto Rico 00931, United States

[‡]Crystallization Design Institute, Molecular Sciences Research Center, University of Puerto Rico, San Juan, Puerto Rico 00926, United States

[§]Department of Pharmaceutical Sciences, University of Puerto Rico, Medical Sciences Campus, San Juan, Puerto Rico 00936, United States

Abstract

The inadvertent occurrence of polymorphic phase transformations in active pharmaceutical ingredients (APIs) during hot melt extrusion (HME) processes has been claimed to limit the application of this technique. Hence, the control of polymorphism would need to be addressed if there is any prospect of HME to be successfully implemented as an alternative solid dosage formulation strategy in integrated, continuous end-to-end pharmaceutical manufacturing settings. This work demonstrates that flufenamic acid (FFA), one of the most polymorphic APIs known, thus far, can be processed using temperature-simulated HME with polyethylene glycol (PEG) as polymeric carrier. At temperatures above the transition point of FFA forms III and I (42 °C), the induction time of the polymorphic phase transformation is longer than the average reported residence time in conventional HME processes (5 min). Moreover, it was demonstrated that thorough understanding of the thermodynamic and kinetic design space for the PEG-FFA system leads to polymorphic control in the produced crystalline solid dispersions. Ultimately, this investigation helps to gain fundamental understanding of the processing needs of crystalline solid dispersions, which will lead to the broader application of HME as a continuous manufacturing strategy for drug products containing APIs prone to polymorphism, representing about 80% of all APIs.

INTRODUCTION

In recent years, hot melt extrusion (HME) has emerged as an enabling technology for continuous pharmaceutical formulation of complex products into solid dosage forms,[1–6] which, up to the present date, is the most convenient and industrially relevant drug delivery for peroral administration.[1,7] In the most common HME setup, raw materials (mainly a mixture of polymer and active pharmaceutical ingredient, API)[8,9] are forced through a heated barrel with a (co)rotating (twin-)screw where the powder blend is intensively mixed in either the molten or partially molten state[1,6] and moved through a die under controlled conditions, which shapes the melt or melt suspension into films, granules, or pellets of uniform size, shape, and density.[10–13] The benefits and pharmaceutical applications of HME, particularly in the context of continuous manufacturing, have been increasingly documented in publications and patents during the past decade.[1,4–6,8,11–18] Moreover, various drug products formulated by extrusion have been approved and marketed in the United States, Europe, and Asia over the past 15 years.[8,10,11,13,17]

HME processes have been reported to produce two types of pharmaceutical formulations with respect to the solid state (amorphous or crystalline) of the API embedded in a polymeric carrier, known as a solid dispersion.[6,9,13] Recent studies demonstrated the feasibility of HME as an alternative continuous formulation strategy to produce crystalline solid dispersions, while improving the dissolution of APIs, an advantage often attributed to amorphous solid dispersions.[1,2,4,6,19–21] Additionally, crystalline solid dispersions present a viable alternative to their amorphous counterparts due to their enhanced stability.[5,6,11,12,17,21–24] Yet, the full potential of crystalline solid dispersions has not been achieved possibly due to the lack of understanding of how the crystalline state behaves during the conditions required for HME, particularly those APIs prone to polymorphic phase transformations.

To date, aside from thermal stability, the polymorphic stability of an API is thought to be a prerequisite when HME is employed to produce solid dosage pharmaceutical formulations.[8,10,13,14,16,25] Polymorphism, a phenomenon that enables molecules to exhibit multiple crystalline phases, is one of the most scrutinized critical quality attributes during the manufacturing of solid dosage formulations.[26,27] Polymorphism is estimated to occur in up to 80% of molecules that display pharmaceutical applications,[27,28] affecting properties of the solid state (stability, solubility, dissolution rate, and bioavailability), and therefore, the quality and efficacy of the final drug product.[24,26,27,29–32] The unsubstantiated notion that undesired polymorphic phase transformations might occur during HME limits the application of this technique to produce crystalline solid dispersions for a narrow set of APIs that are both thermally stable and monomorphic (~20%).[27,28] However, taking into consideration other industrial processes, this sentiment might be founded on insufficient knowledge of the thermodynamic and kinetic boundaries, in other words, the design space of a particular HME process.[12,33–35]

The present study aims to understand polymorphic phase transformations occurring during the production of crystalline solid dispersions by decoupling the effect of critical process parameters (CPPs) that accompany a HME process (temperature, composition, and residence

time) to relate them to the polymorphic outcome of the formulated product.[7,36–40] Other relevant CPPs such as pressure, shear stress, and their combination[8,16,17,41] with temperature, composition, and residence time will be explored in future investigations. Since conventional laboratory hot melt extruders (1) do not allow the independent study of CPPs,[12] (2) require considerable quantities (10–800 g/h) of materials per experiment,[12,41] and (3) do not permit in *situ* monitoring along the process, this work probed the effect of CPPs on the polymorphic phase transformations of physical mixtures using a combination of polarized optical hot-stage microscopy (HSM), offline powder X-ray diffraction (PXRD), and in *situ* time-resolved PXRD. Such an approach served to identify correlations among the selected CPPs and, therefore, will help to minimize the number of experiments needed to be tested in future laboratory-scale HME processes.[12]

In this study, physical mixtures of the model compounds flufenamic acid (FFA) and polyethylene glycol (PEG) were exposed to temperature-simulated HME (TS-HME) processes. The temperatures were chosen above the melting points of the three different PEGs employed (average molecular weights of 4000, 10 000, and 20 000 with melting points of 58.2 °C, 61.6 °C, and 61.9 °C, respectively), but below the temperatures of the liquidus line, thus, where FFA III remained in the solid form. The resulting melt suspension enabled the study of the polymorphic phase transformation of FFA III to FFA I occurring as a result of the selected CPPs during TS- HME.[1,4,5] Particular attention was paid to the induction time of the transformation to determine if a crystalline solid dispersion containing FFA III (metastable under conditions above 42 °C) could be processed in TS-HME experiments enabled by a thorough understanding of the design space for the various PEG-FFA III systems. Ultimately, this investigation helps to gain fundamental understanding of the processing needs of crystalline solid dispersions, which will lead to the broader application of HME as a continuous manufacturing strategy for drug products containing APIs prone to polymorphic phase transformations.

MATERIALS AND METHODS

Materials.

Flufenamic acid (FFA I, 97%) was recrystallized from methanol (ACS reagent, 99.8%), both purchased from Sigma-Aldrich (St. Louis, MO), to produce FFA III as previously described in the literature.[42] Polyethylene glycols (PEGs, 100%) with average molecular weights of 4000, 10 000, and 20 000 were acquired from Alfa Aesar (Ward Hill, MA). All chemicals were used "as received" without further purification.

Sample Preparation.

Physical mixtures of FFA III with the desired PEG were obtained by gently grinding 10 wt % to 80 wt % of FFA III in the various average molecular weights PEGs, respectively, using a mortar with pestle at ambient conditions in the absence of a solvent for 5 min.

Powder X-ray Diffraction (PXRD).

Powder X-ray diffTactograms were collected at 300 K using a Rigaku XtalLAB SuperNova single microfocus Cu Kα radiation (λ = 1.5417 Å) source equipped with a HyPix3000 X-

ray detector in transmission mode operating at 50 kV and 1 mA. Powder samples were mounted in MiTeGen microloops. Powder diffractograms were collected over an angular 2θ range between 6° and 60° with a step size of 0.01° using the fast phi experiment for powders. Data was analyzed within the CrystallisPro (Rigaku) software v 1.171.3920a.

Time-resolved (TR)-PXRD was performed using a Bruker D8 Discover microdiffractometer with the General Area Detector Diffraction System (GADDS) equipped with a VÅNTEC-2000 2D detector and an Anton Paar DCS 350 domed cooling stage. The X-ray beam was monochromated with a graphite crystal (λ Cu Kα = 1.54178 Å, 40 kV, 40 mA). The two-dimensional (2D) diffraction data collection was controlled by the GADDS software. The temperature profiles started at 25 °C with a heating rate of 20 °C/min up to the target temperature (between 70 and 100 °C). Once the 30 min holding time has passed the samples were cooled to 25 °C at rate of 20 °C/min. The diffractograms were recorded prior to the beginning of the temperature profile at 25 °C, respectively, to confirm the phase purity (FFA III) of the sample prior to the start of the experiment. Once the appropriate temperatures were reached, diffractograms were recorded in a 300 s time interval. The scans were acquired with equal incident angle (θ_1) and detector angle (θ_2) at 9°, respectively, under continuous oscillatory movement of the cooling stage in the XY direction (1 mm). One-dimensional diffraction patterns were generated by integrating the 2D XRD data using XRD2EVAL in the Bruker PILOT (v 2014.11–0) software.

Differential Scanning Calorimetry (DSC).

DSC was performed using a DSC TA Q2000 equipped with a RCS40 single-stage refrigeration system and autosampler. The calibration of the instrument was made with an indium standard (T_m = 156.6 °C and H_f = 28.54 J/g). Samples were analyzed by PXRD, to confirm the phase purity (FFA III) in the powder blends prior to the start of the sample preparation for DSC measurement. Samples (approximately 2.000 mg) were prepared using a XP26 microbalance from Mettler Toledo (±0.002 mg) and placed in hermetically sealed aluminum pans equilibrated at 25 °C for 10 min prior to heating to 150 °C under N2 atmosphere (50 mL/min) at a rate of 5 °C/min and temperature accuracy of 0.1 °C. The eutectic temperature and melting point were determined as peak temperatures during the first heating[43,44] and measured at least in duplicate to construct the experimental phase diagram. Data were analyzed with TA Universal Analysis software v 4.5A.

Thermogravimetric Analysis (TGA).

Thermographs were recorded in a TGA Q500 (TA Instruments Inc.) calibrated with calcium oxalate monohydrate. Samples (2–10 mg) were equilibrated at 25 °C for 10 min prior to heating to 150 °C under N_2 atmosphere (60 mL/min) at a rate of 5 °C/min. Additionally, TGAs were performed at three different temperatures, namely, 70 °C, 85 °C, and 100 °C, with a holding time of 60 min under N_2 atmosphere (60 mL/ min), and a heating rate of 20 °C/min. Samples were analyzed by PXRD, to confirm the phase purity (FFA III) in the powder blends prior to TGA measurements. Data was analyzed with TA Universal Analysis software v 4.5A.

Temperature-Simulated HME (TS-HME).

Hot-stage microscopy (HSM) was used to simulate the temperature that would be typically employed in a HME process (TS-HME). The TS-HME was conducted utilizing a polarized optical microscope (Nikon Eclipse LV100N POL) equipped with a temperature controlled hot-stage (Linkam Scientific Instruments Ltd., LTS 420). The hot-stage was calibrated measuring the melting point of water. Pictures were recorded with a Nikon DS-Fi2 camera. Further details of the TS-HME are provided in the Supporting Information. Samples were analyzed by PXRD, to confirm the phase purity (FFA III) in the powder blends prior to TS-HME measurements. The physical mixtures were evenly distributed onto microscope slides and equilibrated at 25 °C prior to the heating (20 °C/min) to the respective target temperature (between 65 and 100 °C). The residence time at the target temperatures was set from 5 to 30 min. Afterward, the samples were cooled down to 25 °C at a cooling rate of 20 °C/min. The microscope slides were then placed in a Petri dish, covered, and stored under 0% humidity in a desiccator filled with P_2O_5 for 24 h before further solid-state characterization was conducted.

Raman Spectroscopy.

Raman spectra were collected using a Raman Microscope (DXR 2, Thermo Fisher Scientific) equipped with a 532 nm laser, 900 lines/mm grating, 25 μm slit, 1 s exposure time with averaging 32 scans, and a RenCam CCD detector. Spectra were collected in a range of 100–3500 cm^{-1} and analyzed using OMNIC software (v 9.2.98).

RESULTS AND DISCUSSION

FFA possesses nine polymorphs, eight of which have been structurally characterized;[45] however, only forms I (FFA I) and III (FFA III) are stable under ambient conditions and readily accessible by conventional solvent methods.[42] These polymorphs are enantiotropically related, with FFA III being the thermodynamically stable form at room temperature, while FFA I is stable above 42 °C.[46] Although FFA I is the commercial form of FFA, FFA III has been chosen as the desired polymorphic form for this study, as it represents the majority of commercial drug products where the APIs are formulated in the thermodynamically most stable polymorph at ambient conditions.[29,47] Physical mixtures (10 wt % to 80 wt %) of FFA III in PEG 4000, 10 000, and 20 000, respectively, were analyzed by PXRD to confirm that the energy input of the sample preparation and storage conditions had no adverse effect on the desired polymorphic form (FFA III) before any experiments were performed (Supporting Information).[26,27] It was concluded that within the detection limits of the PXRD employed, no traceable transformation had occurred. Moreover, preprocessed physical mixtures of FFA III with PEG 4000, PEG 10 000, and PEG 20 000 were stable upon storage for at least 549, 963, and 957 days, respectively (Supporting Information).

The binary eutectic phase diagrams for the PEG-FFA III systems were experimentally derived using DSC to determine the thermodynamic design space needed to process crystalline solid dispersions in the TS-HME experiments (Figure 1 and Supporting Information). The eutectic temperature was selected from the first endothermic event

observed in the DSC thermograms of the physical mixtures, while the second event was utilized to determine the temperature of the liquidus line. The area highlighted in Figure 1 represents the thermodynamic design space, in which PEG 10 000 is molten and FFA III remains in its crystalline form. The TS-HME experiments were conducted within this area on the right side of the eutectic composition (x = 0.40), above the eutectic temperature (51.7 °C), but below the liquidus line for the PEG 10 000-FFA III system (Figure 1). The binary eutectic phase diagrams for the PEG 4000-FFA III and PEG 20 000-FFA III systems are presented in the Supporting Information.

Additionally, the dynamic thermal stability was investigated by TGA employing the same temperature profile utilized when deriving the phase diagrams. For the majority of the physical mixtures the decomposition corresponded to less than 5% weight loss at temperatures between 100 and 150 °C (Supporting Information). Consequently, the temperatures used in the TS-HME were selected taking into account both the phase diagrams (Figure 1 and Supporting Information) and the decomposition observed at temperatures 100 °C (Supporting Information) for all three PEG-FFA III systems. Based on these results and considering that the recommended temperatures for HME should be at least 5–10 °C above the experimentally determined melting point of the polymers (58.2 °C, 61.6 °C, and 61.9 °C for PEG 4000, 10 000, and 20 000, respectively) temperatures employed in the TS-HME ranged from 65 to 100 °C depending on the PEG-FFA III system studied. To address the possible decomposition caused by exposure to elevated temperatures over prolonged time, the thermal stability of pure FFA III as well as the PEGs were studied at selected temperatures (70 °C, 85 °C, and 100 °C) for a total residence time of 60 min (Supporting Information). The maximum residence time for the TS-HME was constrained to 30 min, where only about 0.5% weight loss (indicating decomposition)[27] of FFA III at 100 °C was observed (Supporting Information), which represents six times the average reported maximum residence time in HME processes (5 min).[12,41] The different PEGs depicted negligible weight losses of <0.2%, which are associated with the possible loss of adhered water molecules (Supporting Information).

Raman spectroscopy was employed for phase identification of the different crystal morphologies observed during the TS-HME experiments (Figure 2). The prism-like crystals possessed characteristic Raman shifts at 785, 685, and 524 cm^{-1}, while needle-like crystals presented distinct shifts at 748 and 615 cm^{-1} that matched the reference Raman spectra of FFA I (bottom) and FFA III (top) recrystallized from methanol[42] and employed in the sample preparation of the physical mixtures, respectively.[46] Therefore, it was concluded that the needle-like morphology corresponds to FFA III, while the prism-like morphology corresponds to FFA I.

A representative set of time-lapse micrographs is shown in Figure 3, which depicts the transformation of FFA III (needles) into FFA I (prisms) at the expense of the surrounding FFA III needle-like crystals during the heating (red line) and isotherm (black line) sections of the temperature profile employed for this TS-HME experiment (Figure 3A–D). Figure 3E depicts the commonly observed overgrowth of the translucent surface of FFA I crystals which occurred upon cooling (blue line). These results suggest that a phase transformation

from FFA I back to FFA III (the thermodynamically stable form below 42 °C)[46] might have occurred in the PEG-FFA III systems upon cooling.

The induction time for the polymorphic phase transformation of FFA III into FFA I was determined using in situ polarized HSM and temperature resolved PXRD (TR-PXRD) as well as offline PXRD. The temperature profile employed was identical for the physical mixtures analyzed by each of these techniques. The time elapsed before the appearance of the first FFA I crystal at a particular constant temperature was defined as the induction time for the transformation for the in situ polarized HSM experiments (e.g., 2 min in Figure 3C).

Figure 4 shows the powder diffractograms for a 20 wt % PEG 10 000 (80 wt % FFA III) physical mixture after exposure to a TS-HME at selected constant temperatures. No polymorphic phase transformation was detected at 70 °C after 30 min residence time (Figure 4A). Powder diflractograms of the physical mixture exposed to a temperature of 85 °C (Figure 4B) show the appearance of a diffraction peak (red arrow near 24.4° in 2θ) as the residence time progresses, indicating that a phase transformation has started to occur (20 min). The emergent peak is characteristic of FFA I.[48] The time elapsed before the first observed deviation from the powder diffractogram of FFA III[45] in the powder diffractograms of the PEG-FFA III mixtures was considered as the induction time for the transformation of FFA III to FFA I. The results for other FFA III physical mixtures with PEG 10 000 as well as PEG 4000 and PEG 20 000 are presented in the Supporting Information.

Figure 5 summarizes these measurements and indicates that generally the average induction time decreases with increasing temperature.[42] Basic exponential expressions have been used to calculate the trend lines with the best possible fit for each data set. While physical mixtures containing 60 wt % FFA III were outside of the design space when exposed to temperatures 85 °C (Figure 1), physical mixtures of 80 wt % FFA III exposed to temperatures <80 °C depicted no polymorphic phase transformation during the 30 min residence time (Figure 5A). Considering the extended trend lines in Figure 5A as references, the average induction time increases by a factor of 2.4 when the FFA III content in the physical mixtures is increased from 60 to 80 wt %. Experiments performed with 100 wt % of FFA III show no polymorphic phase transformation when exposed to 100 °C (Supporting Information) for 30 min. These results indicate that the polymorphic phase transformation of FFA III is solvent-mediated, with PEG acting as a solvent leading to partial dissolution of the metastable FFA III and nucleation of the stable FFA I at temperatures above 42 °C. Moreover, with increasing thermodynamic driving force (temperature difference above the transition point of 42 °C) the phase transformation will be faster.[26,27,49,50] Unfortunately, it is rather difficult to determine the solubility of APIs in high molecular weight polymers due to the high viscosity, low molecular mobility, and low vapor pressure of both API and polymer.[51] However, in an effort to demonstrate the impact of the solubility of FFA III in PEG on the phase transformation kinetics, the induction time was measured using PEGs of average molecular weight 4000, 10 000, and 20 000 at various temperatures (Figure 5B).[51] It is hypothesized that an increase in the average molecular weight of PEG would lead to an increase in the induction time, due to the inability of the polymer to dissolve FFA. Figure 5B demonstrates that increasing the average molecular weight of PEG increases the induction time for the polymorphic phase transformation of FFA III to FFA I at a composition of 60 wt

% FFA III. Specifically, the induction time increases by a factor of 4.8 from PEG 4000 to PEG 20 000. These results hint at the possibility of formulating crystalline solid dispersions of the stable form of FFA, FFA III, in PEG even when this form is metastable under the process conditions employed in the TS-HME. Here, the solubility of the API in the polymeric carrier guided through specific polymer—drug interactions[52] might play a role in controlling the polymorphic outcome of the API processed in TS-HME,[53,54] an aspect that will be investigated in future studies.

In Figure 5C it can be observed that the induction times measured by offline PXRD are generally increased by a factor of 4.6 compared to in situ HSM, suggesting that the transformation of FFAIII into FFA I takes longer to occur. Possible explanations for the difference between the induction times measured could be attributed to (l) the in situ versus offline analysis and/or (2) the sensitivity of each technique. To determine the root of the discrepancy, additional in situ TR-PXRD experiments were performed (Figure 5C). The induction times measured by TR-PXRD fall in between those measured by HSM and PXRD. Therefore, it is speculated that the difference in the induction time measured for the transformation of FFA III into FFA I (Figure 5C) occurs as a consequence of the time elapsed prior to the analysis of the physical mixtures, in other words, if the induction time was detected in situ (HSM, TR-PXRD) or offline (PXRD). These results emphasize the importance of process analytical technology for in situ monitoring of polymorphic phase transformations during simulated as well as large-scale HME processes.[3,41,55–61] Moreover, it confirms that the PEG 10 000- FFA III mixtures underwent a transformation from FFA I back to FFA III (thermodynamically stable form) after cooling and storage for 24 h at 0% humidity prior to the PXRD (Figure 3E and Supporting Information). Thus, the induction time for the transformation from FFA III to FFA I was detected later in the experiments analyzed by offline PXRD. Results for physical mixtures with a FFA III content <80 wt % (PEG 10 000 >20 wt %) could not be determined by TR-PXRD due to the high amount of molten PEG, which hampered the detection of the diffraction peaks expected for FFA III present in the samples.

In addition, comparison of the induction times measured by HSM and TR-PXRD, both in situ, indicate that the sensitivity of these techniques also plays a role (Figure 5C). While PXRD measures several thousands of crystals at once and requires a higher quantity of bulk material to be transformed in order to detect the change (generally 0.5% to 10% of the total sample),[26,27,62] HSM depends on the observation of only one FFA I crystal to determine the induction time. This difference in sensitivity might have also contributed to the observed discrepancy between the induction time measured by these two in situ techniques in Figure 5C.

Generally, it can be stated that for all physical mixtures and PEGs employed, the induction times measured with PXRD, the preferred method for phase identification,[27] are longer than the average reported maximum residence time of 5 min for HME (highlighted area in Figure 5C and Supporting Information).[12,41] Combined, these results support the possibility of producing crystalline solid dispersions of pharmaceutical substances prone to displaying polymorphic phase transformations even when the desired polymorph is metastable under the process conditions required for HME. Moreover, the TS-HME physical mixtures of FFA

III with PEG 4000, PEG 10 000, and PEG 20 000 were stable up to the point when this manuscript was submitted, which corresponds to at least 85, 88, and 25 days, respectively (Supporting Information). Although, further investigations are needed to gain deeper understanding of the complex interplay between composition, temperature, pressure, shear stress, and polymer–API interactions occurring during HME processes, the results presented here advance the current understanding for the processing needs of crystalline solid dispersions during HME, particularly those containing APIs prone to polymorphic phase transformations.

CONCLUSIONS

This investigation demonstrates that it is possible to produce crystalline solid dispersions of a nonsteroidal anti-inflammatory drug well-known to display polymorphism via a kinetically controlled process by regulating the composition, temperature, and residence time as well as materials attributes such as the average molecular weight of the polymer. It was established that FFA III (metastable under conditions above 42 °C) could be processed in TS-HME experiments by thorough understanding of the design space for the PEG-FFA III system. This study emphasizes that pharmaceutical substances prone to displaying polymorphic phase transformation might be ultimately formulated using polymer-based extrusion processes[8,13] considering that the average residence time reported for HME amounts to 5 min.[12,41] This conclusion is drawn in light of the results presented above obtained from TS-HME studies, which consider only composition, temperature, residence time, and average molecular weight of the polymer. Other HME relevant parameters such as pressure, shear stress, and their combination with composition, temperature, residence time, as well as type and molecular weight of the polymeric carrier will be explored in future investigations to gain deeper mechanistic understanding of the complex interplay among critical material attributes, CPPs, as well as interactions between the polymer and API that control polymorphic phase transformations in extruded crystalline solid dispersions.

Supplementary Material

Refer to Web version on PubMed Central for supplementary material.

ACKNOWLEDGMENTS

REFERENCES

(1). Baumgartner R; Eitzlmayr A; Matsko N; Tetyczka C; Khinast J; Roblegg E Nano-Extrusion: A Promising Tool for Continuous Manufacturing of Solid Nano-Formulations. Int. J. Pharm. 2014, 477, 1–11. [PubMed: 25304093]

(2). Khinast JG; Baumgartner R; Roblegg E Nano-Extrusion: A One-Step Process for Manufacturing of Solid Nanoparticle Formulations Directly from the Liquid Phase. AAPS PharmSciTech 2013, 14, 601–604. [PubMed: 23463263]

(3). Markl D; Wahl PR; Menezes JC; Koller DM; Kavsek B; Francois K; Roblegg E; Khinast JG Supervisory Control System for Monitoring a Pharmaceutical Hot Melt Extrusion Process. AAPS PharmSciTech 2013, 14, 1034–1044. [PubMed: 23797304]

(4). Mascia S; Heider PL; Zhang H; Lakerveld R; Benyahia B; Barton PI; Braatz RD; Cooney CL; Evans JMB; Jamison TF; Jensen KF; Myerson AS; Trout BL End-to-End Continuous Manufacturing of Pharmaceuticals: Integrated Synthesis, Purification, and Final Dosage Formation. Angew. Chem., Int. Ed. 2013, 52, 12359–12363.

(5). Thommes M; Ely DR; Carvajal MT; Pinal R Improvement of the Dissolution Rate of Poorly Soluble Drugs by Solid Crystal Suspensions. Mol. Pharmaceutics 2011, 8, 727–735.

(6). Desai PM; Hogan RC; Brancazio D; Puri V; Jensen KD; Chun J-H; Myerson AS; Trout BL Integrated Hot-Melt Extrusion - Injection Molding Continuous Tablet Manufacturing Platform: Effects of Critical Process Parameters and Formulation Attributes on Product Robustness and Dimensional Stability. Int. J. Pharm. 2017, 531, 332–342. [PubMed: 28844899]

(7). Ierapetritou MG; Ramachandran R Process Simulation and Data Modeling in Solid Oral Drug Development and Manufacture; Humana Press, 2016.

(8). Crowley MM; Zhang F; Repka MA; Thumma S; Upadhye SB; Kumar Battu S.; McGinity JW; Martin C Pharmaceutical Applications of Hot-Melt Extrusion: Part I. Drug Dev. Ind. Pharm. 2007, 33, 909–926. [PubMed: 17891577]

(9). Aho J; Edinger M; Botker J; Baldursdottir S; Rantanen J Oscillatory Shear Rheology in Examining the Drug-Polymer Interactions Relevant in Hot Melt Extrusion. J. Pharm. Sci. 2016, 105, 160–167. [PubMed: 26852851]

(10). Breitenbach J Melt Extrusion: From Process to Drug Delivery Technology. Eur. J. Pharm. Biopharm. 2002, 54, 107–117. [PubMed: 12191680]

(11). Janssens S; Van den Mooter G Review: Physical Chemistry of Solid Dispersions. J. Pharm. Pharmacol. 2009, 61, 1571–1586. [PubMed: 19958579]

(12). Kolter K; Karl M; Gryczke A Hot-Melt Extrusion with BASF Pharma Polymers — Extrusion Compendium, 2nd ed.; BASF, 2012.

(13). Shah S; Maddineni S; Lu J; Repka MA Melt Extrusion with Poorly Soluble Drugs. Int. J. Pharm. 2013, 453, 233–252. [PubMed: 23178213]

(14). Repka M. a.; Battu SK; Upadhye SB; Thumma S; Crowley MM; Zhang F; Martin C; McGinity JW Pharmaceutical Applications of Hot-Melt Extrusion: Part II. Drug Dev. Ind. Pharm. 2007, 33, 1043–1057. [PubMed: 17963112]

(15). Tho I; Liepold B; Rosenberg J; Maegerlein M; Brandl M; Fricker G Formation of Nano/micro-Dispersions with Improved Dissolution Properties upon Dispersion of Ritonavir Melt Extrudate in Aqueous Media. Eur. J. Pharm. Sci. 2010, 40, 25–32. [PubMed: 20172027]

(16). Djuris J; Nikolakakis I; Ibric S; Djuric Z; Kachrimanis K Preparation of carbamazepine—Soluplus® Solid Dispersions by Hot-Melt Extrusion, and Prediction of Drug—polymer Miscibility by Thermodynamic Model Fitting. Eur. J. Pharm. Biopharm. 2013, 84, 228–237. [PubMed: 23333900]

(17). Hwang I; Kang C-Y; Park J-B Advances in Hot-Melt Extrusion Technology toward Pharmaceutical Objectives. J. Pharm. Invest. 2017, 47, 123–132.

(18). Thiry J; Krier F; Ratwatte S; Thomassin JM.; Jerome C; Evrard B Hot-Melt Extrusion as a Continuous Manufacturing Process to Form Ternary Cyclodextrin Inclusion Complexes. Eur. J. Pharm. Sci. 2017, 96, 590–597. [PubMed: 27687637]

(19). Pietrzak K; Isreb A; Alhnan MA A Flexible-Dose Dispenser for Immediate and Extended Release 3D Printed Tablets. Eur. J. Pharm. Biopharm. 2015, 96, 380–387. [PubMed: 26277660]

(20). Dierickx L; Saerens L; Almeida A; De Beer T; Remon JP; Vervaet C Co-Extrusion as Manufacturing Technique for Fixed-Dose Combination Mini-Matrices. Eur. J. Pharm. Biopharm. 2012, 81, 683–689. [PubMed: 22504402]

(21). Park JB; Kang CY; Kang WS; Choi HG; Han HK; Lee BJ New Investigation of Distribution Imaging and Content Uniformity of Very Low Dose Drugs Using Hot-Melt Extrusion Method. Int. J. Pharm. 2013, 458, 245–253. [PubMed: 24157343]

(22). Kawabata Y; Yamamoto K; Debari K; Onoue S; Yamada S Novel Crystalline Solid Dispersion of Tranilast with High Photo-stability and Improved Oral Bioavailability. Eur. J. Pharm. Sci. 2010, 39, 256–262. [PubMed: 20038453]

(23). Baghel S; Cathcart H; O'Reilly NJ Polymeric Amorphous Solid Dispersions: A Review of Amorphization, Crystallization, Stabilization, Solid-State Characterization, and Aqueous Solubilization of Biopharmaceutical Classification System Class II Drugs. J. Pharm. Sci. 2016, 105, 2527–2544. [PubMed: 26886314]

(24). Bauer JF Polymorphism—A Critical Consideration in Pharmaceutical Development, Manufacturing, and Stability. J. Valid. Technol 2008, 15–23.

(25). Thiry J; Krier F; Evrard B A Review of Pharmaceutical Extrusion: Critical Process Parameters and Scaling-Up. Int. J. Pharm.2015 479, 227–240. [PubMed: 25541517]

(26). Brittain HG Polymorphism in Pharmaceutical Solids, 2nd ed.; Informa Healthcare, USA, Inc.: New York, 2009.

(27). Hilfiker R Polymorphism; Wiley-VCH Verlag GmbH & Co. KGaA: Weinheim, Germany, 2006.

(28). Hamaed H; Pawlowski JM; Cooper BFT; Fu R; Eichhorn SH; Schurko RW Application of Solid-State 35Cl NMR to the Structural Characterization of Hydrochloride Pharmaceuticals and Their Polymorphs. J. Am. Chem. Soc. 2008, 130, 11056–11065. [PubMed: 18656917]

(29). Singhal D; Curatolo W Drug Polymorphism and Dosage Form Design: A Practical Perspective. Adv. Drug Delivery Rev. 2004, 56, 335–347.

(30). U.S. Food and Drug Administrative (FDA) Guidance for Industry - ANDAs: Pharmaceutical Solid Polymorphism, Chemistry, Manufacturing, and Controls Information; U.S. Department of Health and Human Services, 2007.

(31). Peterson ML; Hickey MB; Zaworotko MJ; Almarsson Ö Expanding the Scope of Crystal Form Evaluation in Pharmaceutical Science. J. Pharm. Pharm. Sci. 2006, 9, 317–326. [PubMed: 17207415]

(32). Savjani KT; Gajjar AK; Savjani JK Drug Solubility: Importance and Enhancement Techniques. ISRN Pharm. 2012, 2012, 1–10.

(33). Lai T-TC; Ferguson S; Palmer L; Trout BL; Myerson AS Continuous Crystallization and Polymorph Dynamics in the L -Glutamic Acid System. Org. Process Res. Dev. 2014, 18, 1382–1390.

(34). Johnson MD; May SA; Calvin JR; Remacle J; Stout JR; Diseroad WD; Zaborenko N; Haeberle BD; Sun W-M; Miller MT; Brennan J Development and Scale-Up of a Continuous, High-Pressure, Asymmetric Hydrogenation Reaction, Workup, and Isolation. Org. Process Res. Dev. 2012, 16, 1017–1038.

(35). Singh H Heat Stability of Milk. Int. J. Dairy Technol. 2004, 57, 111–119.

(36). Lionberger R. a.; Lee SL; Lee L; Raw A; Yu LX Quality by Design: Concepts for ANDAs. AAPS J. 2008, 10, 268–276. [PubMed: 18465252]

(37). Food and Drug Administrative (FDA). Guidance for Industry Q8(R2) Pharmaceutical Development; http://www.fda.gov/downloads/Drugs/Guidances/ucm073507.pdf (accessed Sep 28, 2017).

(38). Myerson AS; Krumme M; Nasr M; Thomas H; Braatz RD Control Systems Engineering in Continuous Pharmaceutical Manufacturing. J. Pharm. Sci. 2015, 104, 832–839.

(39). Yu LX; Amidon G; Khan MA; Hoag SW; Polli J; Raju GK; Woodcock J Understanding Pharmaceutical Quality by Design. AAPS J. 2014, 16, 771–783. [PubMed: 24854893]

(40). Robert J-L. Q8(R2): Pharmaceutical Development - ICH; International Conference on Harmonisation of Technical Requirements for Registration of Pharmaceuticals for Human Use; ICH-GCG ASEAN; Kuala Lumpur, Malaysia. 2010.

(41). Patil H; Tiwari RV; Repka MA Hot-Melt Extrusion: From Theory to Application in Pharmaceutical Formulation. AAPS PharmSciTech 2016, 17, 20–42. [PubMed: 26159653]

(42). Gilpin RK; Zhou W Infrared Studies of the Polymorphic States of the Fenamates. J. Pharm. Biomed. Anal. 2005, 37, 509–515. [PubMed: 15740911]

(43). Marinescu DC; Pincu E; Meltzer V Thermodynamic Study of Binary System Propafenone Hydrocloride with Metoprolol Tartrate: Solid-Liquid Equilibrium and Compatibility with a-Lactose Monohydrate and Corn Starch. Int. J. Pharm. 2013, 448, 366–372. [PubMed: 23545398]

(44). Campanella L; Micieli V Solid-liquid Phase Diagrams of Binary Mixtures - Acetylsalicylic acid(1) + E(2) (E 5 Salicylic Acid, Polyethylene Glycol 4000, D-Mannitol). J. Therm. Anal. Calorim. 2010, 99, 887–892.

(45). Lopez-Mejias V; Kampf JW; Matzger AJ Nonamorphism in Flufenamic Acid and a New Record for a Polymorphic Compound with Solved Structures. J. Am. Chem. Soc. 2012, 134, 9872–9875. [PubMed: 22690822]

(46). Hu Y; Wikstrom H; Byrn SR; Taylor LS Estimation of the Transition Temperature for an Enantiotropic Polymorphic System from the Transformation Kinetics Monitored Using Raman Spectros¬copy. J. Pharm. Biomed. Anal. 2007, 45, 546–551. [PubMed: 17851013]

(47). von Raumer M; Dannappel J; Hilfiker R Polymorphism, Salts, and Crystallization - The Relevance of Solid-State Develop¬ment. Chem. Today 2006, 24, 41–44.

(48). Krishna Murthy H. M.; Bhat TN; Vijayan M Structure of a New Crystal Form of 2-{[3-(Trifluoromethyl)phenyl]amino}benzoie Acid (Flufenamie Acid). Acta Crystallogr., Sect. B: Struct. Crystallogr. Cryst. Chem. 1982, 38, 315–317.

(49). Cardew PT; Davey RJ The Kinetcs of Solvent-Mediated Phase Transformations. Proc. R. Soc. London Ser. A 1985, 398, 415–428.

(50). Dette SS; Stelzer T; Rombach E; Jones MJ; Ulrich J Controlling the Internal Diameter of Nanotubes by Changing the Concentration of the Antisolvent. Cryst. Growth Des. 2007, 7, 1615–1617.

(51). Baird JA; Taylor LS Evaluation and Modeling of the Eutectic Composition of Various Drug-Polyethylene Glycol Solid Dispersions. Pharm. Dev. Technol. 2011, 16, 201–211. [PubMed: 20141502]

(52). Zhu Q; Harris MT; Taylor LS Modification of Crystallization Behavior in Drug/polyethylene Glycol Solid Dis¬persions. Mol. Pharmaceutics 2012, 9, 546–553.

(53). Curcio E; Lopez-Mejias V; Di Profio G; Fontananova E; Drioli E; Trout BL; Myerson AS Regulating Nucleation Kinetics through Molecular Interactions at the Polymer-Solute Interface. Cryst. Growth Des. 2014, 14, 678–686.

(54). Lopez-Mejias V; Myerson AS; Trout BL Geometric Design of Heterogeneous Nucleation Sites on Biocompatible Surfaces. Cryst. Growth Des. 2013, 13, 3835–3841.

(55). Food and Drug Administrative (FDA). Guidance for Industry PAT: A Framework for Innovative Pharmaceutical Development, Manufacuring, and Quality Assurance; https://www.fda.gov/downloads/drugs/guidances/ucm070305.pdf (accessed Sep 28, 2017).

(56). Yu LX; Lionberger RA; Raw AS; D'Costa R; Wu H; Hussain AS Applications of Process Analytical Technology to Crystallization Processes. Adv. Drug Delivery Rev. 2004, 56, 349–369.

(57). De Beer T; Burggraeve A; Fonteyne M; Saerens L; Remon JP; Vervaet C Near Infrared and Raman Spectroscopy for the in-Process Monitoring of Pharmaceutical Production Processes. Int. J. Pharm. 2011, 417, 32–47. [PubMed: 21167266]

(58). Saerens L; Dierickx L; Lenain B; Vervaet C; Remon JP; Beer T. De. Raman Spectroscopy for the in-Line Polymer-Drug Quantification and Solid State Characterization during a Pharmaceutical Hot-Melt Extrusion Process. Eur. J. Pharm. Biopharm. 2011, 77, 158–163. [PubMed: 20933084]

(59). Krier F; Mantanus J; Sacre PY; Chavez PF; Thiry J; Pestieau A; Rozet E; Ziemons E; Hubert P; Evrard B PAT Tools for the Control of Co-Extrusion Implants Manufacturing Process. Int. J. Pharm. 2013, 458, 15–24. [PubMed: 24148661]

(60). Wahl PR; Treffer D; Mohr S; Roblegg E; Koscher G; Khinast JG Inline Monitoring and a PAT Strategy for Pharmaceutical Hot Melt Extrusion. Int. J. Pharm. 2013, 455, 159–168. [PubMed: 23911343]

Author Manuscript Author Manuscript Author Manuscript Author Manuscript

(61). Lee SL; O'Connor TF; Yang X; Cruz CN; Chatterjee S; Madurawe RD; Moore CMV; Yu LX; Woodcock J Modernizing Pharmaceutical Manufacturing: From Batch to Continuous Production. J. Pharm. Innov. 2015, 10, 191–199.

(62). Martins Santos O. M.; Dias Reis ME; Tavares Jacon J.; de Sousa Lino ME; Simoes JS; Doriguetto AC Polymorphism: An Evaluation of the Potential Risk to the Quality of Drug Products from the Farmacia Popular Rede Propria. Braz. J. Pharm. Sci. 2014, 50, 1–24.
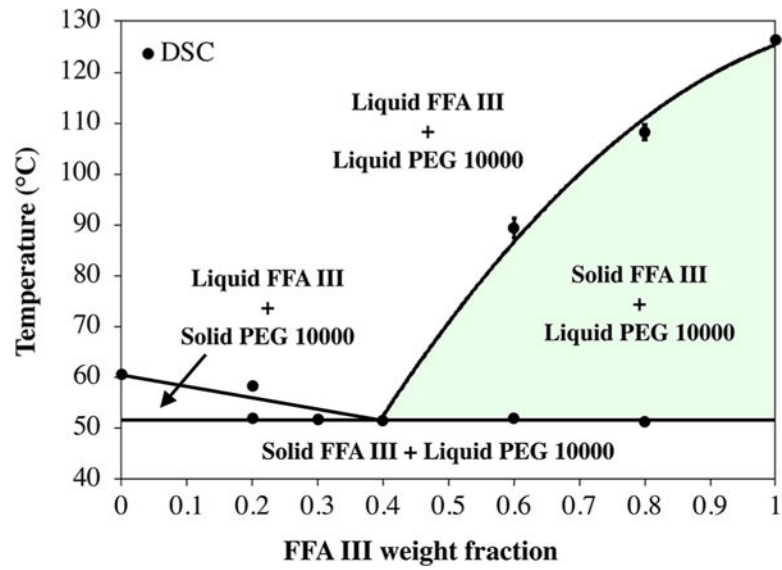
Figure 1.
Phase diagram for the PEG 10 000-FFA III system. Data points (DSC), solid lines (trend lines of experimental DSC data), and highlighted area (thermodynamic design space). If the error bars are not visible they are hidden behind the data points.
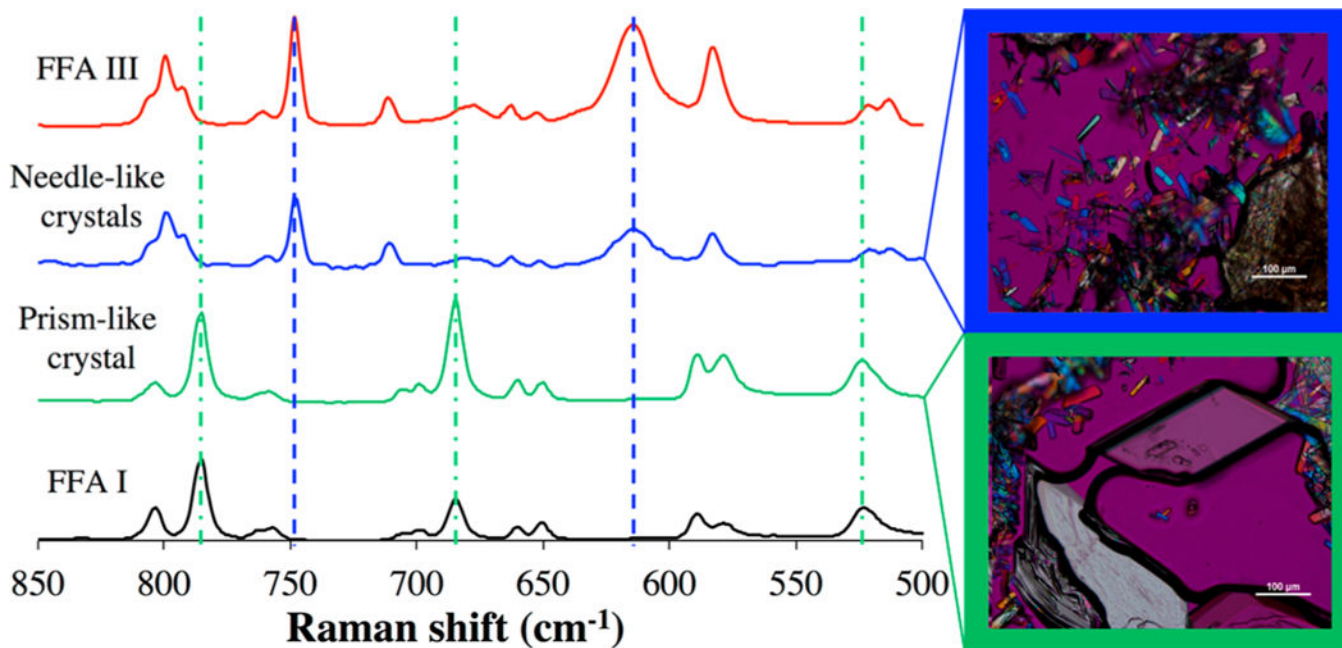

Figure 2.
Raman spectra of "as received" commercial FFA I (black), prism-like crystals obtained after exposure of physical mixture (20 wt % PEG 10 000, 80 wt % FFA III) at 85 °C for 24 h (green), needle-like crystals that remained after exposure (blue), and FFA III employed in sample preparation of physical mixtures (red). Optical micrographs depict needle-like (top right) and prism-like morphologies (bottom right) observed during TS-HME experiment. The scale bars correspond to 100 μm.
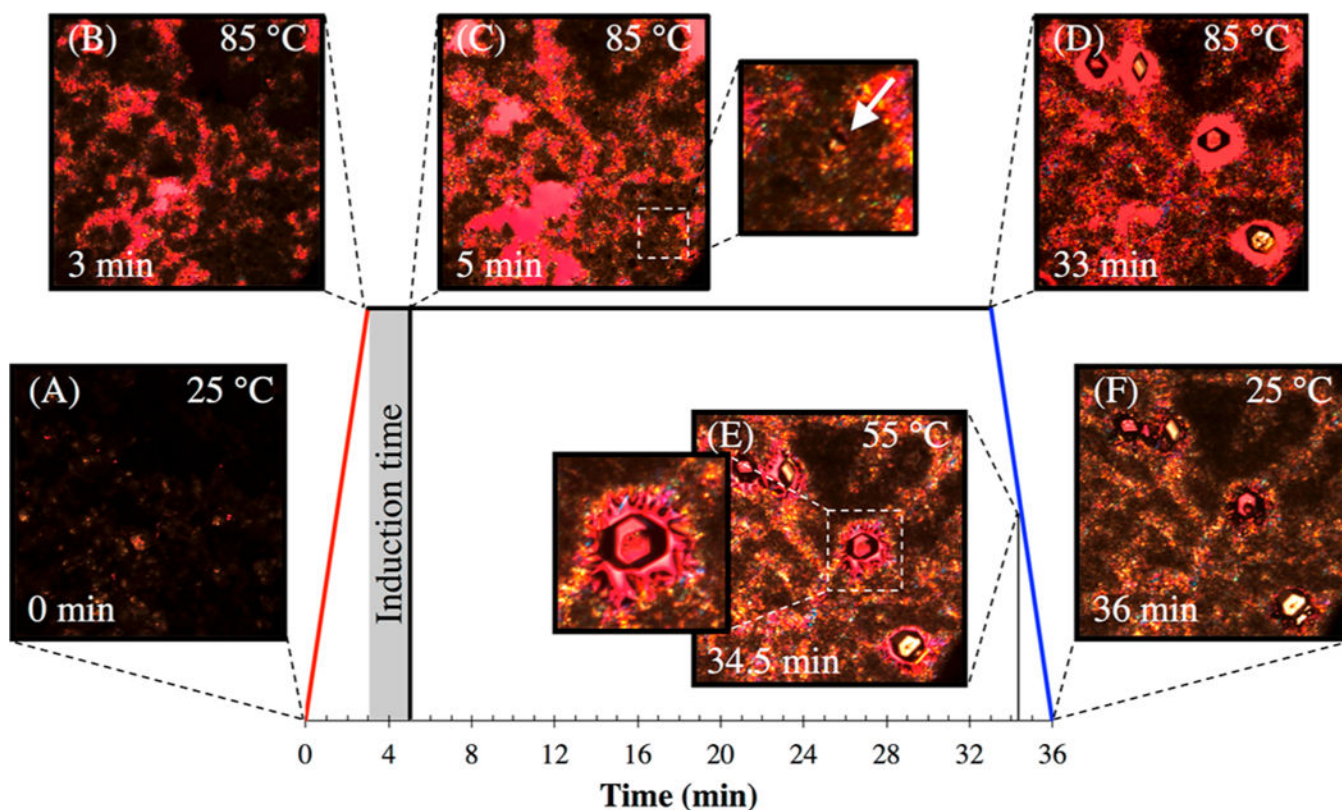
Figure 3.
Time-lapse polarized optical micrographs for a 40 wt % PEG 10 000 (60 wt % FFA III) physical mixture undergoing a TS-HME: (A) before the experiment ($T = 25.0$ °C); (B) at 3.0 min upon reaching a constant temperature of 85.0 °C, PEG 10 000 is molten, and FFA III remained crystalline; (C) at 5.0 min the first prism-like FFA I crystal appeared (white arrow); (D) at 33.0 min the prism-like crystals grew larger; (E) at 34.5 min ($T = 55.0$ °C) the needle-like FFA III crystals grew in the vicinity and on top of the FFA I crystals (white square); and (F) at the end of experiment, 36.0 min ($T = 25.0$ °C). Possible crystal movements during micrograph collection are caused by thermal convection from molten polymer.
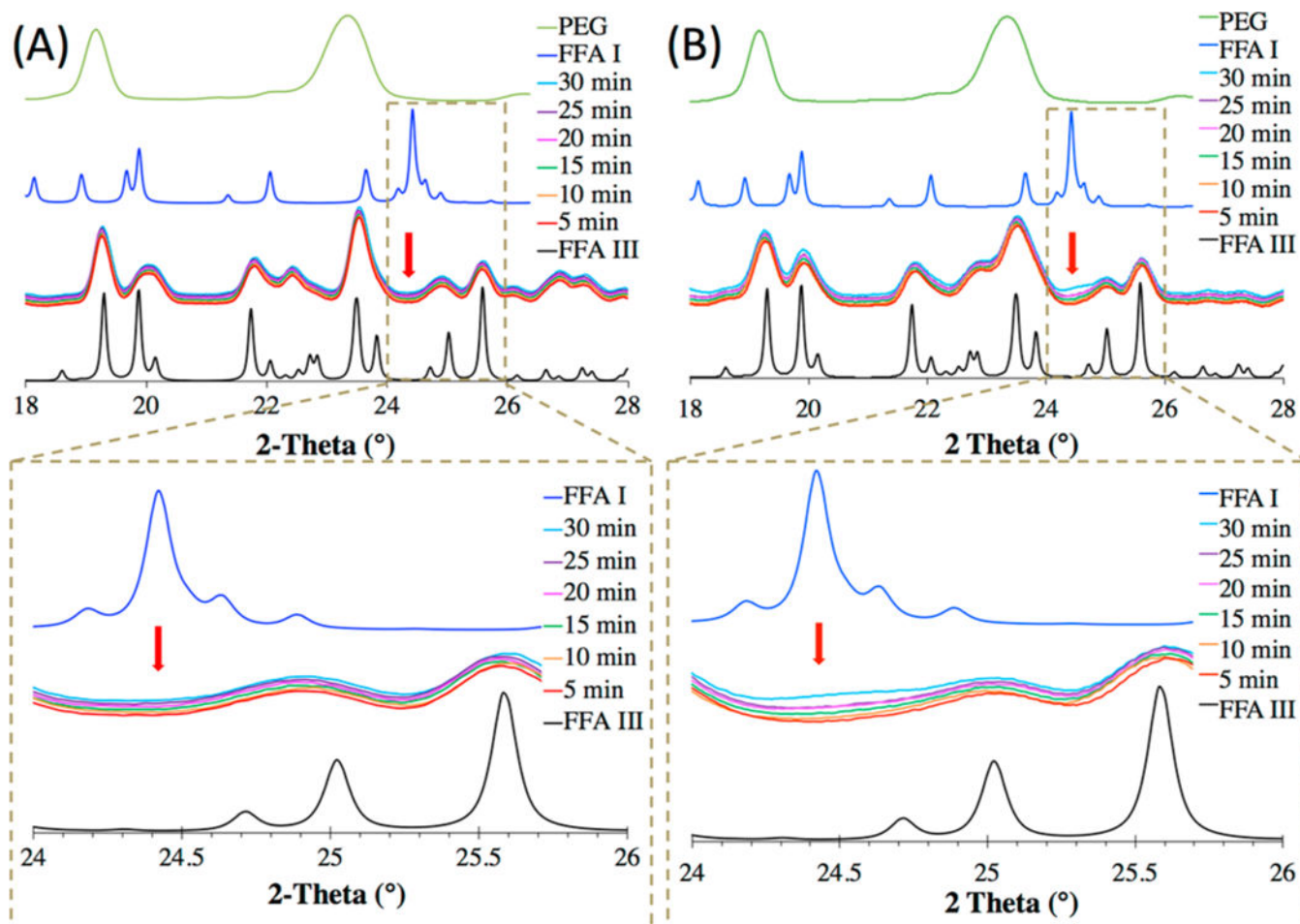
Figure 4.
Powder X-ray diffractograms of a 20 wt % PEG 10 000 (80 wt % FFA III) physical mixture after exposure to TS-HME processes at (A) 70 °C and (B) 85 °C with different residence times and after 24 h storage at 0% humidity. From bottom to top: simulated FFA III (Reference Code, FPAMCA)[45] obtained from the Cambridge Structural Database, CSD (black), physical mixtures processed in TS-HME (various colors), simulated FFA I (Reference Code, FPAMCA11)[48] obtained from CSD (blue) and PEG 10 000 (green).
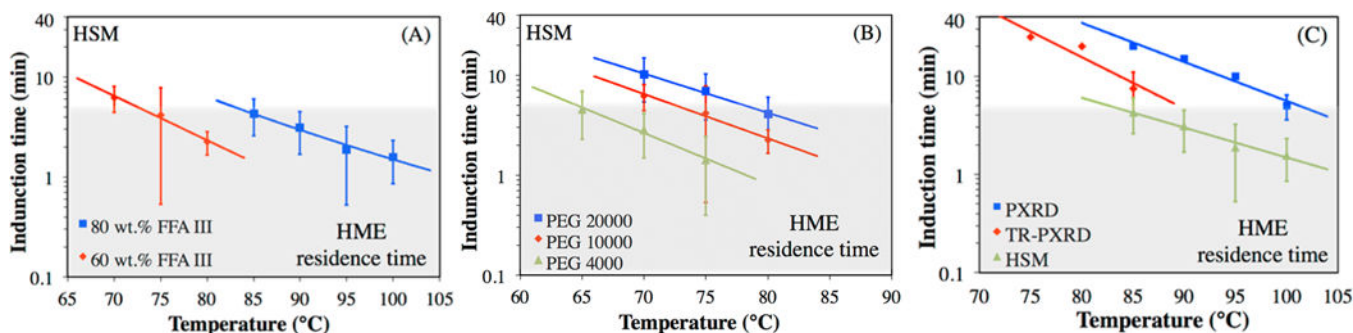
Figure 5.
Average induction time of phase transformation of FFA III into FFA I during TS-HME experiments as a function of (A) FFA III weight fraction in PEG 10 000 (measured in situ by polarized HSM), (B) average molecular weight of PEG for the 60 wt % FFA III composition (measured in situ by polarized HSM), and (C) measuring technique (in situ HSM, TR-PXRD, and offline PXRD) for 80 wt % FFA III in PEG 10 000. Data shown represent the average of at least five measurements for HSM and PXRD and in duplicate for TR-PXRD. If error bars are not visible they are too small and covered by the symbol for the data point. Area highlighted on the bottom of (A–C) indicates the average reported maximum residence time of 5 min for HME.[12,41]